A Model of Excitation and Adaptation in Bacterial Chemotaxis

David C. Hauri and John Ross
Department of Chemistry, Stanford University, Stanford, California 94305 USA

ABSTRACT We present a model of the chemotactic mechanism of *Escherichia coli* that exhibits both initial excitation and eventual complete adaptation to any and all levels of stimulus ("exact" adaptation). In setting up the reaction network, we use only known interactions and experimentally determined cytosolic concentrations. Whenever possible, rate coefficients are first assigned experimentally measured values; second, we permit some variation in these rate coefficients by using a multiple-well optimization technique and incremental adjustment to obtain values that are sufficient to engender initial response to stimuli (excitation) and an eventual return of behavior to baseline (adaptation). The predictions of the model are similar to the observed behavior of wild-type bacteria in regard to the time scale of excitation in the presence of both attractant and repellent. The model predicts a weaker response to attractant than that observed experimentally, and the time scale of adaptation does not depend as strongly upon stimulant concentration as does that for wild-type bacteria. The mechanism responsible for long-term adaptation is local rather than global: on addition of a repellent or attractant, the receptor types not sensitive to that attractant or repellent do not change their average methylation level in the long term, although transient changes do occur. By carrying out a phenomenological simulation of bacterial chemotaxis, we find that the model is insufficiently sensitive to effect taxis in a gradient of attractant. However, by arbitrarily increasing the sensitivity of the motor to the tumble effector (phosphorylated CheY), we can obtain chemotactic behavior.

INTRODUCTION

Second-messenger signaling and phosphorylation cascades are extremely important mechanisms for eukaryotic regulation and response. However, such systems are generally explained qualitatively at best, and few explicit models solved numerically have been made to quantify and test our understanding of the mechanisms involved. One system that is understood in enough detail to allow for the construction of a biochemical mechanism is the chemotactic mechanism of coliform bacteria such as *Escherichia coli* and *Salmonella typhimurium*. Chemotaxis in these bacteria has been studied extensively: a variety of experiments have been reported as well as theoretical studies and formulations of biochemical kinetic reaction mechanisms (Berg and Purcell, 1977; Block et al., 1982; Hess et al., 1988; Kuo and Koshland, 1989; Matsumura et al., 1990; Ninfa et al., 1991; Stewart and Dahlquist, 1987; Stock et al., 1991).

One of the outstanding features of bacterial chemotaxis is that it exhibits "exact" adaptation. By this we mean that if a bacterium is exposed to a stepwise change in the chemical makeup of its environment (an increase in the concentration of the attractant serine, for example), it will first undergo excitation as it responds to this change and temporarily alters its behavior, but it will eventually undergo exact adaptation whereby its behavior returns completely to the pre-stimulus behavior (Berg and Tedesco, 1975; Spudich and Koshland, 1975). This is as opposed to the partial adaptation seen in systems such as vision where the system adapts to changes in input light intensity over a wide range, but does not adapt completely (Dowling and Ripps, 1970).

To understand chemotaxis in *E. coli* and to be able to make predictions, it is important to have a model that accounts for the observed phenomena (i.e., excitation, adaptation, etc.) within the parameters set by the reactions, concentrations, and species observed in the chemotactic mechanism. Previously, Bray et al. (1993) modeled the reactions taking part in chemotactic excitation. Their thorough treatment of the subject reproduces bacterial excitation quite well, although they experience difficulty in accounting for the observed sensitivity to attractant. They do not attempt, however, to incorporate adaptation into their model. In this work we present a new model of chemotaxis in *E. coli* that seeks to account for adaptation as well as excitation by using reactions that have been described in the literature but never treated quantitatively, and by making use of a formalism described by Segel et al. (Knox et al., 1986; Segel et al., 1986). We test the reasonableness of this model by incorporating it into a phenomenological model of chemotaxis in three dimensions and comparing the results with observations of living bacteria.

In Background we briefly review the biochemistry of chemotaxis in *E. coli*. We then present in The Model the reaction mechanism used in our model to simulate the signaling pathway and equations used to simulate chemotaxis in three dimensions. In the section so titled, we present the Results and Discussion of the predictions of the model, including excitation and a full return to basal response after the addition of changing levels of concentrations of attractant, repellent, and any combination of the two. We also present our simulations of bacterial chemotaxis, from which we determine that by increasing the sensitivity to attractant we can obtain chemotaxis similar to that seen in experiments. In Concluding Remarks we discuss the areas of agreement and disagreement between our model and experiments.

Received for publication 1 September 1994 and in final form 14 November 1994.

Address reprint requests to Dr. John Ross, Department of Chemistry, Stanford University, Stanford, CA 94305. Tel.: 415-723-9203; Fax: 415-723-4817; E-mail: ross@chemistry.stanford.edu.

0006-3495/95/02/708/15 $2.00

In previous work we have addressed the issue of the implementation of logic gates, Turing machines, and neural network (parallel) machines by means of macroscopic chemical kinetics (Arkin and Ross, 1994; Hjelmfelt and Ross, 1992, 1993; Hjelmfelt et al., 1993, 1991, 1992). We return to this subject in the presentation of the results by comparing the chemotactic mechanisms to a sophisticated adding machine.

BACKGROUND

Lacking a steering or explicit guiding mechanism, coliform bacteria rely upon a biased random walk to move up gradients of attractants and down gradients of repellents, such that when they are moving in a favorable direction (toward attractant or away from repellent) they continue swimming smoothly for a greater period of time, on average, than when they are swimming in an unfavorable direction. In both cases "runs" (periods of smooth swimming) are terminated by "tumbles" that serve to randomize the direction in which the bacteria are swimming (Berg and Brown, 1972; Berg and Tedesco, 1975; Larsen et al., 1974; Silverman and Simon, 1974; Spudich and Koshland, 1975; Stock et al., 1991). *E. coli* have an average of six helical flagella (Leifson, 1960), and the swimming behavior (i.e., whether a bacterium is running or tumbling) is determined by an interaction of these flagella. Clockwise (CW) rotation of the flagella leads to tumbling, and counterclockwise (CCW) rotation leads to smooth swimming (Larsen et al., 1974; Macnab, 1977; Macnab and Aizawa, 1984; Macnab and Ornston, 1977).

In the absence of attractant or repellent, the flagella of tethered *E. coli* tend to spin CCW about 65% of the time (Block et al., 1982; Kuo and Koshland, 1989), and we refer to this as the basal activity. We define the word activity to be the quantitative measure of the signal sent from a receptor complex to the motor. Thus, the statement that a given receptor complex has an activity of 0.65 indicates that if all receptor complexes were in the same signaling state as the receptor complex in question, a flagellum would spin CCW 65% of the time. It is important to distinguish this number, the percentage of time an individual flagellum rotates CCW, from the percentage of time a multiply flagellated bacterium spends swimming smoothly, about 80% in the absence of stimuli (Berg and Brown, 1972). The two measures differ because at any given time some of the flagella might be rotating CCW and others CW, and the percentage of time spent swimming smoothly depends upon an interaction of these flagella. The mechanism of interaction is complicated and not well understood, as flagella can, for example, invert their screw-sense under strain. A "voting hypothesis" has been suggested where there is a threshold number of flagella that must rotate CW for the bacterium to tumble (Ishihara et al., 1983; Weis and Koshland, 1990). It is also not clear that the CCW bias is the same for tethered *E. coli* as it is for free swimming bacteria, because the torque at the motor is significantly different in the two cases.

Fig. 1 illustrates the reactions that are currently understood to be involved in the biochemical pathway leading to this behavior. In the presence of ATP, the kinase CheA undergoes

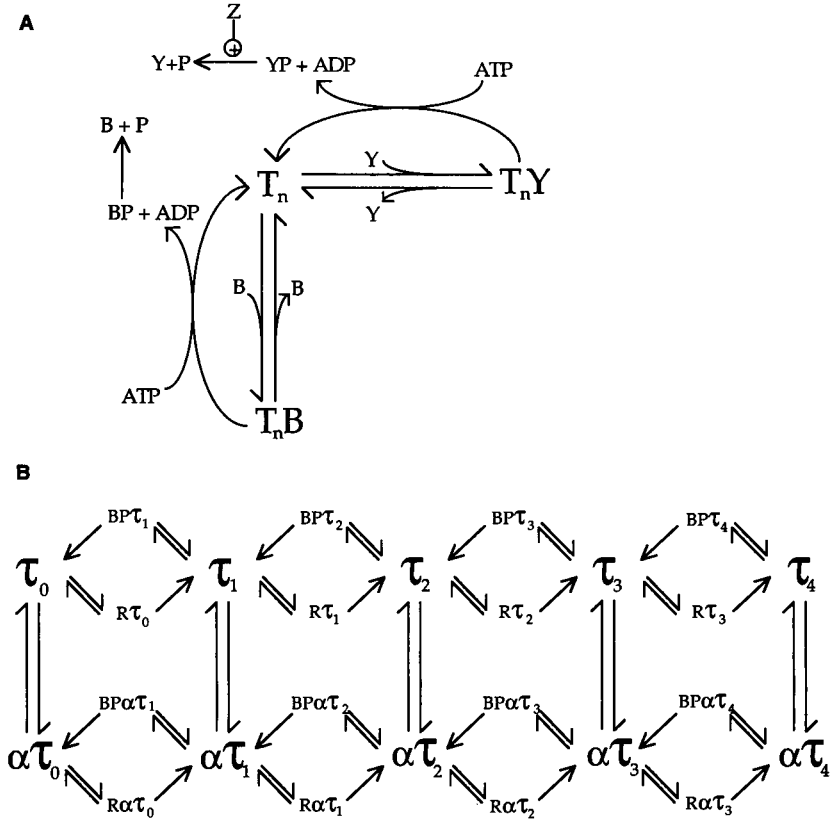

FIGURE 1 Chemical reactions of our model of bacterial chemotaxis. (*A*) Phosphorylation pathways. T stands for the transmembrane receptor complex (composed of receptor, CheW, and CheA), B for CheB, Y for CheY, Z for CheZ, P for a phosphoryl group, and *n* for the methylation state of the receptor. The rate of the phosphorylation reactions depends upon the state of methylation of the receptor and whether an external ligand is bound. These states are shown schematically in *B*. The reactions shown in *A* are those that affect the rate of phosphoryl group transfer from the kinase CheA (part of the receptor complex T) to either Y or B. (*B*) We combine the three receptor complexes shown in *A* (T_n, T_nB, and T_nY), and define this unit as τ_n. Thus, for example, τ_2 stands for the combination of species T_2, T_2Y, and T_2B. All three of these species have the same rates for the reactions shown in *B*, so we do not differentiate between them. R stands for CheR, and α for attractant. As we move to the right in this figure, the rate of phosphorylation increases, leading to a decrease in activity; as we bind α the rate of phosphorylation decreases, which leads to a decrease in activity.

autophosphorylation that is accelerated by CheW and a receptor such as Tar or Tsr (formerly referred to as methylating chemotaxis proteins) (Borkovich et al., 1989; Borkovich and Simon, 1990; Hess et al., 1988; McNally and Matsumura, 1991; Ninfa et al., 1991). Although there is probably some free CheA in the cytoplasm, studies have indicated that CheA, CheW, and receptors form a complex with a half-life on the order of 7 min (Russell et al., 1989; Schuster et al., 1993). This interval is significantly longer than the time scale of excitation and adaptation (less than 1 min for small concentrations). Hence, in Fig. 1 these three species are combined into a complex such as Tar-CheW-CheA that we label T. Generally, the receptor has four sites that can be methylated by the methyltransferase CheR (which we label R) (Borkovich et al., 1992; Engström and Hazelbauer, 1980; Silverman and Simon, 1977; Simms et al., 1987; Terwilliger et al., 1986), and demethylated by the methylesterase CheB (Koshland, 1988; Russell et al., 1989; Stock et al., 1991). The phosphorylated form of CheB (PB) is significantly more active than the dephosphorylated form (B) (Borczuk et al., 1986; Lupas et al., 1983). The methylation state of the receptor (indicated in Fig. 1 by a subscript denoting the number of methyl groups attached to the receptor) has a significant effect upon the kinetics of phosphoryl group transfer from the kinase CheA (part of the complex T) to the substrate, such that as the number of methyl groups bound to a receptor is increased, the rate of phosphorylation at that receptor complex is generally also increased (Borkovich et al., 1992). The receptor-bound kinase can either phosphorylate CheY (Y) or B. Phosphorylated Y (YP) adds cooperatively to the flagellar motor to promote CW rotation (Kuo and Koshland, 1987, 1989; Lukat et al., 1991; Ravid et al., 1986) and is dephosphorylated by the enzyme CheZ (Bourret et al., 1990; Hess et al., 1988; Ravid et al., 1986).

If *E. coli* bacteria are exposed to a step increase of attractant (α) or repellent (ρ), they first exhibit excitation, whereby smooth swimming increases for α, and decreases for ρ (Berg and Tedesco, 1975; Spudich and Koshland, 1975). The change in the CCW bias at the individual flagellar motors is due to a change in the concentration of YP, caused by a change in the rate at which T_n phosphorylates Y (a decrease in the rate of phosphorylation of Y if α binds). This rate change is due to a ligand-induced conformational change in the T_n (Parkinson, 1993; Stewart and Dahlquist, 1987; Stock et al., 1989). After some time (a few seconds for physiologic concentrations), the bacteria adapt to the ambient concentration of attractant or repellent, and if the concentration remains at that level the flagella will resume the basal CCW bias of 0.65 (Berg and Tedesco, 1975; Spudich and Koshland, 1975).

For attractants, two mechanistic pathways have been observed for adaptation, both of which effect adaptation by changing the average methylation state of the receptors, and thereby changing the rate of phosphorylation of Y and possibly B (the same exist for repellent, but the directions of change are reversed): one is a decrease in the rate of demethylation related to a decrease in the concentration of BP (Bourret et al., 1991; Kehry et al., 1984; Kleene et al., 1979; Russell et al., 1989; Sanders and Koshland, 1988; Stewart and Dahlquist, 1987; Toews et al., 1979), and the other an increase in the rate of methylation of a receptor with α bound, where the rate change is due to a conformational change at that receptor (Kehry et al., 1984; Kleene et al., 1979; Silverman and Simon, 1977; Springer et al., 1977; Terwilliger et al., 1986). The first implies a global signal, such that the rate of demethylation changes even for receptors with no ligand bound, whereas the second implies a local signal affecting only individual receptors with ligand bound. Experiments indicate that attractants specific to one type of receptor cause preferential methylation at that receptor type, although they may cause some increased methylation at other receptor types (Silverman and Simon, 1977; Springer et al., 1977), so that a change in BP concentration cannot be the only factor involved in adaptation. Other studies indicate that the rate of demethylation returns to the basal level after complete adaptation, whereas the rate of methylation changes as long as external ligand is bound (Kehry et al., 1984; Terwilliger et al., 1986). Work by Hazelbauer et al. (1989) also suggests that local receptor modification is the major pathway for adaptation, but when this modification is suppressed, global mechanisms can compensate. All of these observations are compatible with a biochemical network in which the concentration of BP increases transiently, but returns to a basal level upon adaptation.[1]

MODEL

Biochemical network

In this study we integrate and expand previous work by presenting what is, to our knowledge, the first quantitative model of the enzyme reactions necessary for excitation and adaptation in bacterial chemotaxis.

Chemotaxis begins with the binding of attractant (α) or repellent (ρ) to a receptor. We assume that the association and dissociation kinetics of a ligand with the receptor are fast compared with those of subsequent reactions, and the concentration of bound attractant obeys the equilibrium equation

$$[\alpha\tau_n] = \frac{\alpha[\tau_n]}{K_D + \alpha}, \quad (1)$$

where K_D is the dissociation constant, α is the concentration of attractant, and τ_n is the concentration of receptors in the nth methylation state, as shown in Fig. 1.

[1] In fact, Silverman and Simon seem to show some global adaptation in that the serine receptor does undergo some increase in methylation in response to aspartate and vice-versa, although the increases are not as large as those seen at the receptor specific to the attractant added. However, this is not necessarily inconsistent with a transient increase in BP followed by a return to a basal level, because a transient change in methylation rate would be expected to show an increase in the number of radiolabeled methyl groups attached to the receptor protein because of the temporary increase in turnover (see experimental methods in Silverman and Simon, 1977).

The biochemical network is illustrated in Fig. 1. Both second messengers Y and B add to the receptor T and can then either dissociate without change or be phosphorylated by phosphate transfer from ATP. The rate phosphorylation depends upon the number of methylesterified glutamate side chains of the receptor (the value of the subscript n, referred to here as the "methylation state") and whether a stimulatory molecule is bound to T. We model the transfer of phosphate from ATP to the second messengers as bimolecular reactions and the dephosphorylation of second messengers as unimolecular reactions (we incorporate the concentration of CheZ, the enzyme responsible for the dephosphorylation of YP, into the rate coefficient and assume that [CheZ] does not change significantly). We use Michaelis-Menten kinetics to model the methylation and demethylation reactions; for the values of V_M and K_M chosen, the enzymes are generally unsaturated. In Fig. 1 *B*, the three species T_n, T_nY, and T_nB are grouped together as τ_n. Attractants and repellents can add to any of these forms, and the K_D is not affected by the methylation state. The presence of stimulatory ligand and the methylation state both affect the rate of methylation of the receptor, whereas only the methylation state affects the rate of demethylation.

The kinetics of the binding of YP to the motor are not well understood. We use the phenomenological observation (Kuo and Koshland, 1989) that the fraction of CCW rotation is related to the concentration of YP according to the equation

$$f_{CCW} = \frac{1}{1 + h(YP)^{5.5}}, \qquad (2)$$

where f_{CCW} is the fraction of time the motor spends rotating CCW, and h is a constant. One effect of our assumption of instantaneous action is that the motor in our model responds more quickly to changes in the YP concentration than if we were to model explicit binding of YP to the motor.

Determination of rate coefficients that confer exact adaptation

The authors are unaware of quantitative experimental work describing the effect of methylation state on the rate of phosphorylation of Y and B. Hence, we focus not on trying to find actual, in vivo values for these rates, but on demonstrating that exact adaptation can exist for some set of physically reasonable rate coefficients.

Segel et al. have developed an incisive formal model of adaptation in a general system involving one modification site (Knox et al., 1986; Segel et al., 1986). We take advantage of their treatment and adapt it to our system of four methylation sites, noting that the order of methylation at the receptor appears to be immaterial (Terwilliger et al., 1986). First, we assume that binding and release of the stimulating ligand (aspartate, for example) is fast compared with interconversion between methylation states, and we simplify the chemotactic machinery to a set of 10 receptor species (the 5 methylation states with attractant bound, and 5 in the unbound state). With each receptor species we associate an activity, a_n, as shown in Fig. 2, and total activity is a linear combination of the individual activities and receptor species concentrations shown in Fig. 2:

$$\mathbf{A} = \sum_{n=0}^{4} (a_n \tau_n + a_{n+5} \alpha\tau_n), \qquad (3)$$

where **A** is total activity and the a_n values are the activities associated with the given receptor species, and $\alpha\tau$ is a receptor with attractant bound. These activities are eventually used to determine the rates of phosphoryl group transfer from the τ_n complexes to Y and B, but first we concern ourselves only with the assumption that they correspond to %CCW rotation at the motor. This assumption allows us to consider only rates of methylation and demethylation in the presence

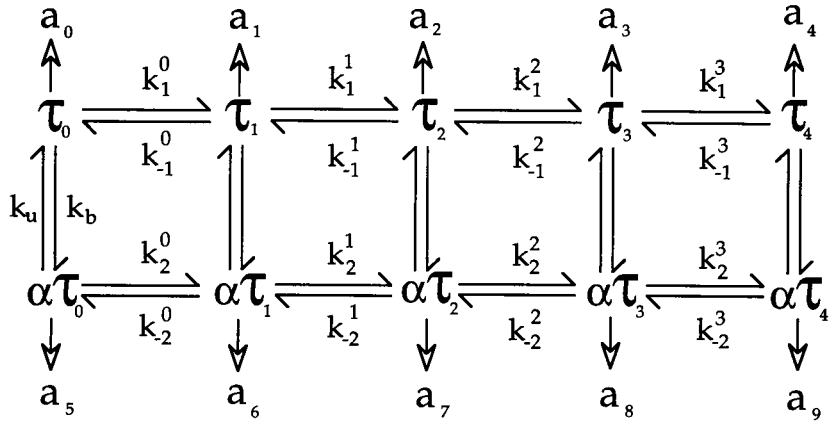

FIGURE 2 Model system used for the calculation of methylation/demethylation rates and activities of receptor complexes. T_n stands for the transmembrane receptor complex, made up of receptor, CheA, and CheW, where the complex is in the nth methylation state; α for attractant; a_n for the activity of the associated receptor complex; k_b and k_u for the rate coefficients of binding and unbinding of attractant, respectively; and the remaining ks for the rate coefficients of methylation and demethylation of receptor complexes. Activity increases upon binding of α to the receptor complexes and decreases going from left to right in the diagram (from low methylation level to high methylation level). After the addition of attractant, some concentration shifts downward (i.e., shifts from the T_n complexes to the αT_n complexes), thereby quickly causing an increase in activity. The ratio of methylation rate to demethylation rate is larger at the bottom of the diagram, so the average methylation state subsequently increases, which thereby causes a slow decrease in activity and thus leads to adaptation.

and absence of α, and the activities of the receptor complexes; for the time being, we ignore all complications related to phosphorylation and competition between Y and B, the changing concentration of BP, and the generation in time of a signal. By looking first at the steady-state behavior, the equations we obtain are not time-dependent, so we can solve them without resorting to time-consuming integration methods, a simplification that makes multivariable optimization techniques manageable. In this way we can solve the equations associated with the simplified system, and then relate these to the complete system.

With no attractant present, the total activity is the basal activity

$$\mathbf{A}_0 = \sum_{n=0}^{4} a_n \tau_n. \tag{4}$$

If we define the quantity β such that

$$\beta = \frac{\mathbf{A}_0}{\sum_{n=0}^{4} (\tau_n + \alpha\tau_n)}, \tag{5}$$

then we can substitute Eq. 4 into Eq. 5 and rearrange to obtain

$$\sum_{n=0}^{4} (a_n - \beta)\tau_n = 0 \tag{6}$$

in the absence of α. If we define

$$\tilde{a}_n = a_n - \beta, \tag{7}$$

then the condition for exact adaptation is that, at steady state,

$$\sum_{n=0}^{4} (\tilde{a}_n T_n + \tilde{a}_{n+5}\alpha\tau_n) = 0. \tag{8}$$

At steady state, we define a quantity J_n (the flux between the two receptor species τ_{n-1} and τ_n) such that

$$J_n = k_1^{n-1}\tau_{n-1} - k_{-1}^{n-1}\tau_n = -(k_2^{n-1}\alpha\tau_{n-1} - k_{-2}^{n-1}\alpha\tau_n), \tag{9}$$

where the second equality holds because we are at steady state (this is equivalent to Kirchoff's current law for electrical circuits). We solve Eq. 9 for the τ_n and $\alpha\tau_n$ species and substitute these values into Eq. 8, to obtain

The six terms in this equation are independent, so for Eq. 10 to be true, always, each term must equal zero. Therefore, Eq. 10 provides us with six separate equations; we use these to help to determine the 10 activities and 16 rate coefficients for methylation and demethylation. We do not explicitly input experimentally determined rates here because we wish to allow the optimization routine as much leeway as possible. The number of independent rate coefficients can be reduced by assuming that the rate of demethylation is not influenced by the binding of attractant (except through a transient change in BP concentration that will be discussed later). The assumption that the average methylation state with no attractant bound is two adds an additional equation, as does the assumption that an increase in methylation level of one methyl group offsets the addition of one attractant ligand (Mowbray and Koshland, 1987; Parkinson, 1993). We then have an underdefined system of 8 equations and 22 unknowns, which can be optimized to obtain the largest value for the objective function

$$\sum_{n=0}^{4} \frac{\tilde{a}_{n+5}}{\tilde{a}_n} \tag{11}$$

consistent with physically reasonable rate coefficients (i.e., all are positive and are bounded above by the rate of diffusion) and activities (i.e., all are positive). The largest value of the above objective function is of interest because, as seen in Fig. 2, when α binds, the activity of the receptor complex changes from a_n to a_{n+5}. Therefore, by maximizing Eq. 11, we maximize the response to added attractant. (Strictly speaking, the above objective function should be maximized with each term weighted by the concentration of τ_n, to get absolute maximum response, but this is difficult and the above function gives quite good results.) We use the continuous simulated annealing global optimization algorithm described by Corana et al. (Corana et al., 1987; Metropolis et al., 1953) in an attempt to avoid being trapped in a local minimum. Once a solution is obtained for the simplified system shown in Fig. 2, where the solution is in the form of (at least) locally optimal rate coefficients and activities all consistent with Eq. 10 and the constraints discussed above, we then add in, piecewise, components of the full system shown in Fig. 1. As a first approximation, we assume that the a_n values obtained can

$$\begin{aligned}
&J_1\left(\frac{\tilde{a}_0}{k_1^0} - \frac{\tilde{a}_5}{k_2^0}\right) + J_2\left(\frac{\tilde{a}_1}{k_1^1} - \frac{\tilde{a}_6}{k_2^1} + \frac{\tilde{a}_0 k_{-1}^0}{k_1^0 k_1^1} - \frac{\tilde{a}_5 k_{-2}^0}{k_2^0 k_2^1}\right) \\
&\quad + J_3\left(\frac{\tilde{a}_2}{k_1^2} - \frac{\tilde{a}_7}{k_2^2} + \frac{\tilde{a}_1 k_{-1}^1}{k_1^1 k_1^2} - \frac{\tilde{a}_6 k_{-2}^1}{k_2^1 k_2^2} + \frac{\tilde{a}_0 k_{-1}^0 k_{-1}^1}{k_1^0 k_1^1 k_1^2} - \frac{\tilde{a}_5 k_{-2}^0 k_{-2}^1}{k_2^0 k_2^1 k_2^2}\right) \\
&\quad + J_4\left(\frac{\tilde{a}_3}{k_1^3} - \frac{\tilde{a}_8}{k_2^3} + \frac{\tilde{a}_2 k_{-1}^2}{k_1^2 k_1^3} - \frac{\tilde{a}_7 k_{-2}^2}{k_2^2 k_2^3} + \frac{\tilde{a}_1 k_{-1}^1 k_{-1}^2}{k_1^1 k_1^2 k_1^3} - \frac{\tilde{a}_6 k_{-2}^1 k_{-2}^2}{k_2^1 k_2^2 k_2^3} + \frac{\tilde{a}_0 k_{-1}^0 k_{-1}^1 k_{-1}^2}{k_1^0 k_1^1 k_1^2 k_1^3} - \frac{\tilde{a}_5 k_{-2}^0 k_{-2}^1 k_{-2}^2}{k_2^0 k_2^1 k_2^2 k_2^3}\right) \\
&\quad + k_{-1}^0 k_{-1}^1 k_{-1}^2 k_{-1}^3 T_4\left(\frac{\tilde{a}_0}{k_1^0 k_1^1 k_1^2 k_1^3} + \frac{\tilde{a}_1}{k_{-1}^0 k_1^1 k_1^2 k_1^3} + \frac{\tilde{a}_2}{k_{-1}^0 k_{-1}^1 k_1^2 k_1^3} + \frac{\tilde{a}_3}{k_{-1}^0 k_{-1}^1 k_{-1}^2 k_1^3} + \frac{\tilde{a}_4}{k_{-1}^0 k_{-1}^1 k_{-1}^2 k_{-1}^3}\right) \\
&\quad + k_{-2}^0 k_{-2}^1 k_{-2}^2 k_{-2}^3 \alpha T_4\left(\frac{\tilde{a}_5}{k_2^0 k_2^1 k_2^2 k_2^3} + \frac{\tilde{a}_6}{k_{-2}^0 k_2^1 k_2^2 k_2^3} + \frac{\tilde{a}_7}{k_{-2}^0 k_{-2}^1 k_2^2 k_2^3} + \frac{\tilde{a}_8}{k_{-2}^0 k_{-2}^1 k_{-2}^2 k_2^3} + \frac{\tilde{a}_9}{k_{-2}^0 k_{-2}^1 k_{-2}^2 k_{-2}^3}\right) = 0.
\end{aligned} \tag{10}$$

TABLE 1 Reactions and rate coefficients used in calculations along with in vitro values

	Reaction	Rate coefficient	Rate coefficient with α bound to T	Rate coefficient with ρ bound to T	Literature value and source
1.	$T_n + Y \rightarrow T_nY$	5 $(\mu M\ s)^{-1}$	Same	Same	4×10^{-4} $(\mu M\ s)^{-1}$ (Schuster et al., 1993)‡
2.	$T_nY \rightarrow T_n + Y$	5 s^{-1}	Same	Same	1×10^{-5} s^{-1} (Schuster et al., 1993)‡
3a.	$T_0Y + ATP \rightarrow T_0 + YP$	0.0472 s^{-1}*	0.0001 s^{-1}*	0.9975 s^{-1}*	Average value without stimulus bound:
3b.	$T_1Y + ATP \rightarrow T_1 + YP$	1.858 s^{-1}*	0.001 s^{-1}*	3.2 s^{-1}*	1×10^{-2} s^{-1} (Schuster et al., 1993)‡
3c.	$T_2Y + ATP \rightarrow T_2 + YP$	1.861 s^{-1}*	0.005 s^{-1}*	3.5 s^{-1}*	Rate coeff. for 3e is ~50 times that for 3a with
3d.	$T_3Y + ATP \rightarrow T_3 + YP$	1.895 s^{-1}*	1.2 s^{-1}*	3.2 s^{-1}*	no stimulus bound (Borkovich et al., 1992)
3e.	$T_4Y + ATP \rightarrow T_4 + YP$	1.901 s^{-1}*	2.1 s^{-1}*	0.9 s^{-1}*	
4.	$T_n + B \rightarrow T_nB$	0.8 $(\mu M\ s)^{-1}$	Same	Same	
5.	$T_nB \rightarrow T_n + B$	1 s^{-1}	Same	Same	
6a.	$T_0B + ATP \rightarrow T_0 + BP$	0.012 s^{-1}*	0.0001 s^{-1}*	0.25 s^{-1}*	Average value without stimulatory ligand bound:
6b.	$T_1B + ATP \rightarrow T_1 + BP$	0.464 s^{-1}*	0.002 s^{-1}*	0.7 s^{-1}*	0.014 s^{-1} (Lupas et al., 1983)
6c.	$T_2B + ATP \rightarrow T_2 + BP$	0.465 s^{-1}*	0.010 s^{-1}*	0.875 s^{-1}*	
6d.	$T_3B + ATP \rightarrow T_3 + BP$	0.474 s^{-1}*	0.413 s^{-1}*	1.0 s^{-1}*	
6e.	$T_4B + ATP \rightarrow T_4 + BP$	0.475 s^{-1}*	0.460 s^{-1}*	0.0625 s^{-1}*	
7.	$YP \rightarrow Y + P$	6 s^{-1}§			10 s^{-1} (Lukat et al., 1991)
8.	$BP \rightarrow B + P$	2 s^{-1}			0.14 s^{-1} (Stock et al., 1989)
		V_{max} (K_m = 13 μM)	V_{max} (K_m = 13 μM)		
9a.	$\tau_0 \rightarrow \tau_1$	10.0 $\mu M\ s^{-1}$	10.3 $\mu M\ s^{-1}$	3 $\mu M\ s^{-1}$	Average value without stimulatory ligand bound:
9b.	$\tau_1 \rightarrow \tau_2$	18.8 $\mu M\ s^{-1}$	38.4 $\mu M\ s^{-1}$	5 $\mu M\ s^{-1}$	3 $\mu M\ s^{-1}$ (Lupas et al., 1983)
9c.	$\tau_2 \rightarrow \tau_3$	35.3 $\mu M\ s^{-1}$	67.2 $\mu M\ s^{-1}$	15 $\mu M\ s^{-1}$	
9d.	$\tau_3 \rightarrow \tau_4$	24.1 $\mu M\ s^{-1}$	36.7 $\mu M\ s^{-1}$	6 $\mu M\ s^{-1}$	
10a.	$\tau_1 \rightarrow \tau_0$	$BP \times 182\ s^1$	Same	Same	Average value for concentrations used in model:
10b.	$\tau_2 \rightarrow \tau_1$	$BP \times 228\ s^{-1}$			$BP \times 0.1\ s^{-1}$ (Terwilliger et al., 1986)
10c.	$\tau_3 \rightarrow \tau_2$	$BP \times 186\ s^{-1}$			
10d.	$\tau_4 \rightarrow \tau_3$	$BP \times 228\ s^{-1}$			

*The concentration of ATP is assumed to be constant and is incorporated into the rate coefficient.

‡If we calculate the maximum rate of phosphorylation of Y from these rates, assuming this is the only major pathway to phosphorylation, then regardless of the specific model, we find that the rates given by this experiment imply a steady-state phosphorylation rate of roughly 10 molecules per second. The binding of attractant to 10% of receptor sites changes this value to 9 molecules per second. It seems unlikely that this rate of phosphorylation can account for the observed behavior (e.g., response within 0.2 s), so we believe that the in vivo rates for these reactions must be significantly faster than the experimentally determined in vitro rates.

§The concentration of CheZ is assumed to be constant and is incorporated into the rate coefficient; it is assumed that this enzyme is operating well below saturation.

be converted into the phosphorylation rates of Y and B by multiplying by an appropriate constant (which is chosen to bring the rates into closer agreement with experimental values and to reproduce behavioral traits). We then adjust rate coefficients concurrently to preserve exact adaptation and reasonable kinetics. When all of the components have been added, the rate coefficients are adjusted a final time to bring them somewhat more into agreement with experimental results and to bring the behavior of the system closer to that observed experimentally, subject to the retention of exact adaptation and a large excitation. Next, we use the same method for the determination of activities and rate coefficients related to repellent binding, where our optimization is now constrained by the formerly determined values for the unbound receptor. We assume that receptors with both α and ρ bound concurrently have the same activities and rate coefficients for methylation and demethylation as receptors with no stimulatory ligands bound.

Table 1 lists each reaction in Fig. 1 and gives the rate coefficients obtained in the manner described, with references to experiments relevant to the determination of the in vivo values. For example, reaction 3b is the phosphorylation and release of Y bound to receptors with one methyl group attached. The rate of this reaction decreases from 1.858 to 0.001 s^{-1} on binding attractant, and increases to 3.2 s^{-1} on binding repellent.

The rates given for methylation and demethylation are the V_{max} values using Michaelis-Menten kinetics at a K_M of 10 μM. For demethylation we use the equation

$$V_{\tau_n \rightarrow \tau_{n-1}} = \frac{V_{max}\,\tau_n(BP)}{10\mu M + \tau_n}. \qquad (12)$$

To facilitate the comparison of this work with that of other researchers, we use the same total concentration of species as Bray et al. (1993) (5 μM τ,[2] 2 μM B, and 10 μM Y), and the same cell volume (1.41×10^{-15} L (Kuo and Koshland, 1987)).

Simulation of chemotactic trajectories

The result of the chemotactic mechanism in bacteria is their movement in a gradient; likewise, the most reasonable test

[2] A referee has kindly pointed out the reference Gegner et al. (1992), which demonstrates that at cytosolic concentrations using Tsr as the receptor, about 30% of the free CheA and CheW are present in the fully formed receptor complex, indicating that the complex concentration we have assumed may be too high by a factor of three. If we lower the concentration of the complex by a factor of 3 we can obtain essentially the same results with reasonable changes in the other parameters.

of a proposed mechanism is to determine whether that mechanism is capable of giving rise to chemotaxis.

To investigate the chemotactic behavior of our model, we simulate bacterial chemotaxis in an infinite, three-dimensional tank. Because the way in which flagella interact to produce smooth or tumbly motion is not well understood, we take values where these interactions are known and extrapolate between points. Experiments indicate that the mean period of a run in the absence of stimuli is 0.86 ± 1.18 s, and the mean tumble period is 0.14 ± 0.19 s (Berg and Brown, 1972). To approximate this distribution of run and tumble periods, we use a memory-less (exponential) function and equate the median of our function with the mean of the experimental value (to adjust slightly for the portion of longer runs observed experimentally), using 100 ms time steps. Let $P(S \mid T)$ indicate the probability of a transition from smooth swimming to tumbling within the next 100 ms. Then, if $P(CCW) = 1$, the bacterium will never tumble, so $P(S \mid T) = 0$, whereas if $P(CCW) = 0$ then $P(S \mid T) = 1$ because the bacterium will always tumble. The probability of CCW rotation in unstimulated *E. coli* is 0.65, and the probability of a transition from a tumble to a run in the next 100 ms is 0.097 (obtained using an exponential distribution with a median of 0.86 s). Therefore, if $P(CCW) = 0.65$ then $P(S \mid T) = 0.097$.

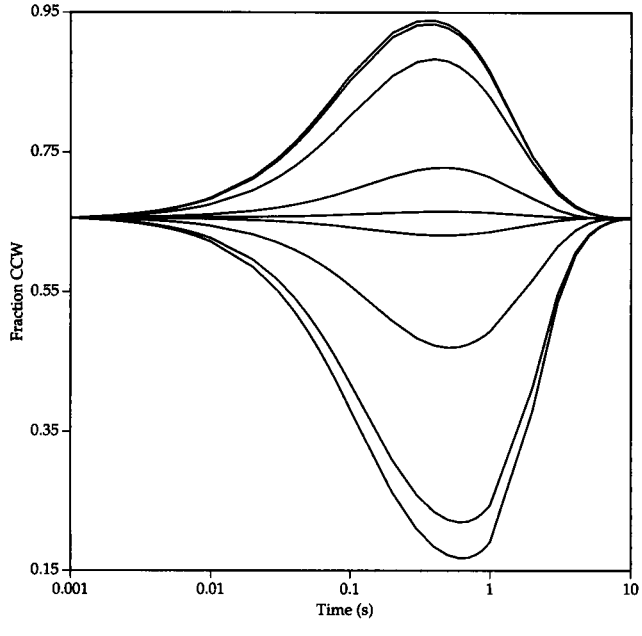

FIGURE 3 Plot of response to addition of attractant and repellent (measured in the fraction of counter clockwise (CCW) rotation of a flagellum) versus time; the response curves show the initial excitation and eventual adaptation of the model to different levels of aspartate (Asp) and Ni^{2+} added at $t = 0$. The concentrations used are (going from the lowest curve to the highest): 10 mM Ni^{2+}, 1 mM Ni^{2+}, 100 μM Ni^{2+}, 10 μM Ni^{2+}, 0.01 μM Asp, 0.1 μM Asp, 1 μM Asp, 10 μM Asp, and 100 μM Asp (note that all curves that show a transient decrease in fraction CCW are for the addition of Ni^{2+}, whereas all curves showing a transient increase in fraction CCW are for the addition of aspartate). The responses show a saturation at high concentrations of stimuli because the receptors become saturated. As shown experimentally (Segall et al., 1986; Tso and Adler, 1974), the model is more sensitive to aspartate than Ni^{2+}.

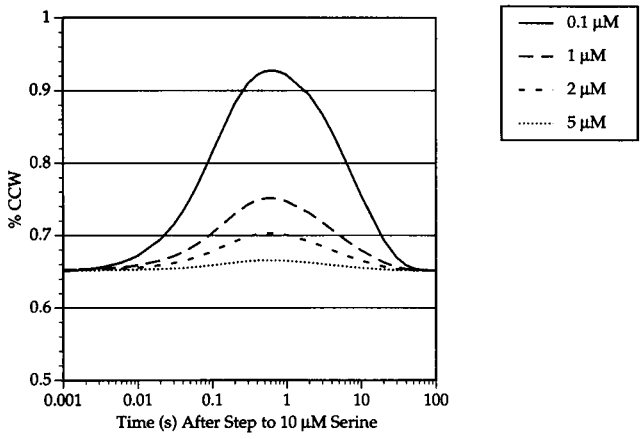

FIGURE 4 Plot of percentage counter-clockwise rotation (CCW) of a flagellum versus time; the response curves show initial excitation and eventual adaptation of the model to 10 μM aspartate added at $t = 0$, after the model has already adapted to the level of aspartate indicated.

Assuming an equation of the form

$$P(S \mid T) = P(CCW)^x, \tag{13}$$

we can now solve for X using the three sets of values described above to obtain

$$P(S \mid T) = P(CCW)^{2.22}, \tag{14}$$

and, similarly, the probability of beginning a run while tumbling obeys the equation:

$$P(T \mid S) = P(CCW)^{0.676}, \tag{15}$$

where $P(T \mid S)$ indicates the probability of a transition from tumbling to smooth swimming. We use these equations to determine the probability at each time point of switching between smooth-swimming and tumbling. This produces a dwell-time histogram for run and tumble lengths that nicely reproduces the linear (major) region of that determined by Kuo and Koshland (1989). We ignore the change in direction during runs (experimentally measured to be an average change in direction of 23 ± 23° (Berg and Brown, 1972)), and we assume a speed of 14.2 μm s^{-1} (Berg and Brown, 1972). We then place a simulated bacterium in three-dimensional space a given distance from a source of aspartate producing a normal distribution (Crank, 1975) of the attractant centered at the origin. Chemotactic ability is determined by the likelihood that the simulated bacterium will remain in the vicinity of the attractant after approximately one-half h (2000 s). The mean change in direction during a tumble is 68 ± 36° (Berg and Brown, 1972), so if our simulated bacterium tumbles, we generate the radial angle from a pseudo-random normal distribution with these properties, and the azimuthal angle from a uniform distribution between 0 and 2π.

All simulations are run on a DECstation 3100. The system of differential equations obtained from the reactions given in Table 1 is integrated with a Backward Differentiation Formula (BDF) and a Newton method, from FORTRAN subroutines provided by the Numerical Algorithms Group

(NAG). Pseudo-random number generators are also part of the NAG FORTRAN library.

RESULTS AND DISCUSSION

Response to step changes in attractant and repellent concentration

Fig. 3 shows the excitation and adaptation of our model to a number of different concentrations of the attractant aspartate, and the repellent Ni^{2+}. We use a K_D for aspartate of 0.5 μM (Foster et al., 1985). The K_D for Ni^{2+} is unknown. We used a value of 200 μM to obtain the experimentally observed response to an increase in the level of this repellent (Tso and Adler, 1974). Saturation for α occurs at around 10 μM, and for ρ at around 10 mM. Experiments demonstrate that *E. coli* are far more sensitive to aspartate than Ni^{2+} (Foster et al., 1985; Segall et al., 1986; Tso and Adler, 1974), and we have included this observation in our model. Fig. 4 shows the excitation and adaptation to the addition of 10 μM aspartate after adaptation to differing aspartate concentrations. The results of the model show quantitative adaptation. The threshold response (5% change in rotational bias) for attractant occurs at about 0.05 μM aspartate. This is a significant result because previous authors have been forced to postulate unobserved reactions to achieve a similar sensitivity (Bray et al., 1993), whereas our model makes use of no such assumptions (we do use a K_D for aspartate of 0.5 μM, instead of 1 μM, so in fact our sensitivity is still somewhat smaller than what the authors achieved by assuming diffusion-limited dephosphorylation of Y by attractant-bound T). Wild-type *E. coli* show a similar response to concentration of aspartate roughly 100 times more dilute (Segall et al., 1986).

Fig. 5 shows the response of the different species in the mechanism to a step increase in aspartate concentration from 0 to 10 μM. Let us look at the entire chemotactic process when α binds to a receptor. First, the conformation of that receptor changes, which decreases the rate of phosphorylation of both Y and B. The decreased concentration of YP

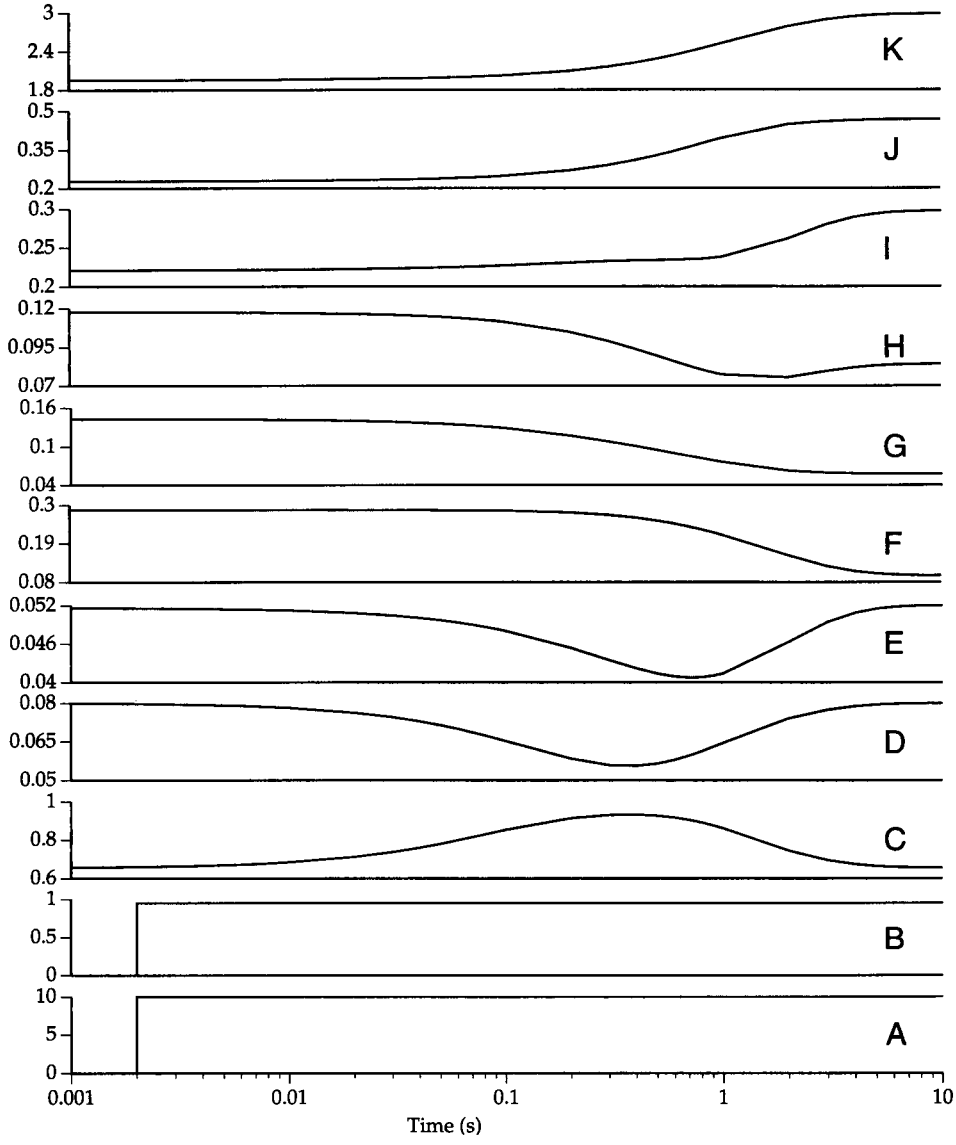

FIGURE 5 Plot of responses of several species of the chemotactic mechanism versus time after the addition of 10 μM aspartate. (*A*) The concentration of aspartate (μM). (*B*) The fraction of receptors with aspartate bound. This value rises to 0.95 immediately after the addition of aspartate at $t = 0.002$. (*C*) The fraction YP/Y_{tot}, where Y_{tot} is the total concentration of all species of Y in the bacterium. (*D*) The percentage CCW bias. This value starts out at the basal level of 0.65 and rises above 0.95 before eventual adaptation. (*E*) The fraction BP/B_{tot}. (*F*) The fraction T_0/T_{tot}; the fraction of receptors in the 0th methylation state (where methylation state is the number of reversible methylation sites per receptor occupied by methyl groups). (*G*) The fraction T_1/T_{tot}. (*H*) The fraction T_2/T_{tot}. (*I*) The fraction T_3/T_{tot}. (*J*) The fraction T_4/T_{tot}. (*K*) The average methylation state. The average methylation state increases after the initial excitation, which leads to adaptation.

leads to an increase in CCW rotation and, hence, to more smooth swimming. Second, the concentration of BP also decreases, which causes a decrease in the rate of demethylation of all receptors. Third, the binding of α to a receptor increases the rate of methylation of that particular protein molecule. In time, the decreased rate of demethylation at all receptors, and the increased rate of methylation at receptors with α bound, lead to an increase in the average methylation level of the receptors. The higher methylation level counteracts the effect of attractant binding by increasing the rate of phosphorylation. As the average methylation increases, the concentrations of YP and BP return to the basal level, and the CCW rotational bias returns to 65%. Further, as the concentration of BP returns to the basal level, the rate of demethylation returns to the basal level also, so that at all receptors except those responsive to the specific attractant added, the steady-state average methylation level returns to the pre-stimulus value. However, the average methylation level at the receptors specific to the attractant approaches a steady-state value that is higher than the pre-stimulus value. This is due to the increase in the rate of methylation at those receptors; all of the receptors specific to that attractant experience a similar influence of the attractant, because attractant binds and unbinds rapidly with the receptor complexes and so spends, on average, the same amount of time bound to each receptor. Thus, we see both excitation and eventual adaptation.

In Fig. 6 we show the maximum excitation to addition or removal of attractant. We first allow the model to adapt to the concentration of aspartate shown on the axis labeled "initial concentration." We then change the concentration of aspartate in a step to the concentration shown on the axis labeled "final concentration." On the third axis, we plot the peak excitation in %CCW as a result of this change in concentration of aspartate. If we increase the level of aspartate, we see a peak excitation at greater than 65% CCW, which indicates a response of an increased fraction of smooth swimming; if we decrease aspartate, the peak excitation is at a value smaller than 65%, because the response is a decrease in the fraction of smooth swimming. In Fig. 7 we show the effects of adding varying concentrations of repellent and attractant concurrently. In Fig. 7 *A* we plot the peak excitation as varying shades of gray versus the fraction of receptors with attractant and repellent bound, whereas Fig. 7 *B* shows a side view of the same graph; the peak excitation is plotted along the vertical axis, and the horizontal axis is the function $f_{asp} - f_{Ni}$, where f_{Ni} is the fraction of receptors with Ni^{2+} bound and f_{asp} is the fraction of receptors with aspartate bound. The

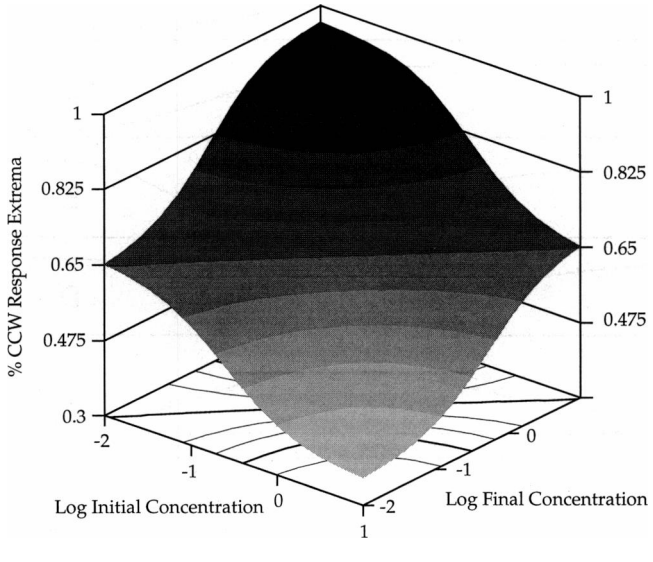

FIGURE 6 Plot of %CCW at the peak of the response versus concentration of aspartate as a function of the initial concentration of aspartate; the model is run at the initial concentration of aspartate shown until adaptation is complete. The aspartate concentration is then changed to the final concentration, and the response is calculated.

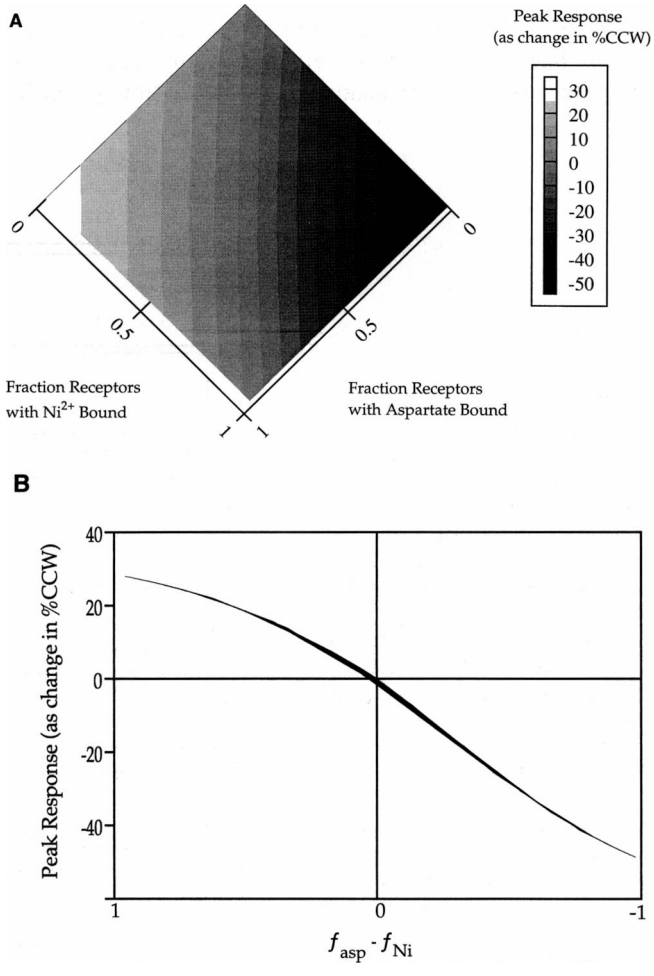

FIGURE 7 Plot of the effect of different concentrations of aspartate and Ni^{2+} (plotted as fraction of receptors with stimulatory ligand bound) on the peak excitation after a step addition of stimulus. (*A*) On one axis is the fraction of receptors with Ni^{2+} bound, on the other is the fraction of receptors with aspartate bound, and the peak excitation after both stimuli have been added simultaneously and in a step increase is shown as the level of gray plotted. (*B*) The peak excitation plotted as a function of the difference between the fraction of receptors with aspartate bound (f_{asp}) and the fraction with Ni^{2+} bound (f_{Ni}). Note that *B* includes all possible combinations of attractant and repellent, and yet approximates a single, slightly sigmoidal line. This indicates that the model predicts the chemotactic mechanism to act as a somewhat nonlinear adder.

lines of equal excitation in A are nearly vertical, indicating that the model predicts that the response mechanism of chemotaxis in *E. coli* acts like a standard, if slightly nonlinear, adding mechanism.

For a step increase in aspartate of roughly 0.1 μM, the peak excitation in our model is reached in about one-half s, and adaptation is complete in less than 10 s. The time of attaining the peak excitation is in rough agreement with observed results (Block et al., 1982), especially given the fact that if we were to include the binding of Y to the motor then we would add a small delay in the peak excitation time and so we would then expect the agreement to be nearly exact. The adaptation time is also reasonable for physiologic concentrations of stimuli: any response lasting more than about 10 s would be meaningless because by that point bacterial motion is completely randomized by Brownian motion and so it would not do a bacterium any good to "remember" concentrations sensed more than 10 s in the past (Berg and Purcell, 1977). A deviation of our model from experimentally observed behavior is seen in the variation in time scales for adaptation to significantly different levels of attractant. Although *E. coli* adapt in less than 5 s to physiologic increases in the concentration of attractant (Block et al., 1982), adaptation time increases with increasing attractant concentrations such that it may take many tens of minutes to adapt to concentrations of attractant that are sufficient to saturate the receptors (Berg and Tedesco, 1975; Segall et al., 1982; Spudich and Koshland, 1975). This may indicate that the methylating and/or demethylating enzymes are operating near saturation and become saturated during adaptation. In our model we assumed that all enzymes are unsaturated.

Fig. 8 illustrates the peak excitation for different concentrations of attractant compared with the final average methylation state of the receptors. The curves are overlain to demonstrate their similarity.

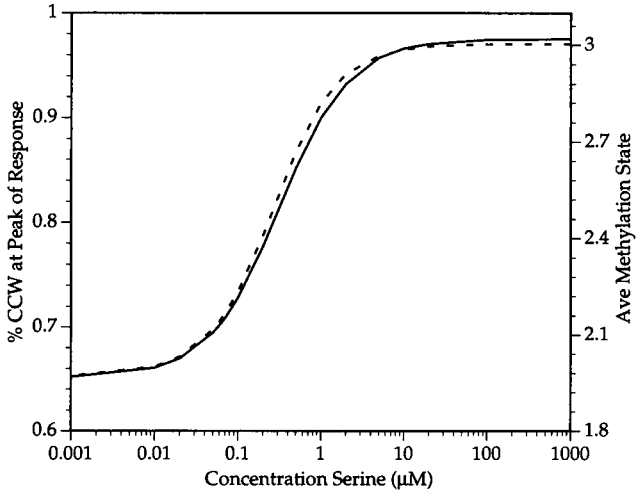

FIGURE 8 Plot of %CCW at peak of excitation and average methylation state versus aspartate concentration, upon the addition of different levels of attractant. The dashed line gives the %CCW reached at the peak of the excitation, and the solid line is the average methylation state of the receptors after complete adaptation.

Dependence of excitation and adaptation on chosen rate coefficients

The effect of changes in rate coefficients on predictions of the model is shown in Fig. 9. The rate coefficients for the reactions shown are doubled (except for the K_M values, which are halved. We halve the K_M values because decreasing the K_M alone brings the enzyme closer to the saturation region, and we are interested in observing the resulting effects). We plot the percentage change in YP concentration in the unstimulated state after this change in rate coefficient. Thus, for example, if the rate of dephosphorylation of YP is doubled (reaction 7), the concentration of YP in the unstimulated state drops to about 90% of its original value, for the rate coefficients used in the model. Also shown is the change in %CCW before addition of and after adaptation to a 10 μM step addition of aspartate. To obtain this value, the constant h in Eq. 2 is adjusted for the new YP concentration (i.e., the value after the indicated rate coefficient has been changed, and the system has reached steady state) such that the basal level of %CCW is 65. Then 10 μM aspartate is added and after adaptation the new level of %CCW is recorded, and the difference between these two values is given in the figure. Looking again at reaction 7, we see that upon doubling the rate coefficient, the adaptation to 10 μM aspartate is not complete, returning to about 68% CCW rather than 65%. In the case where the rates are dependent upon methylation level (for example, reactions 3a through 3e), we simply double all relevant rates at the same time, rather than look at how the rate at each methylation level affects the system. From this figure we see that the concentration of YP is most sensitive to the rate of YP dephosphorylation and YP production, as we expect. Adaptation is most sensitive to the rate of demethylation and the rate of BP production, although surprisingly the rate of methylation is not as significant.[3]

Simulations of chemotaxis

To determine the general chemotactic ability of our model, we ran simulations of bacterial chemotaxis as described in The Model. First, we simulate the random behavior of a bacterium in a stimulus-free environment according to our model. In Fig. 10 A we plot the mean distance from the origin of twelve such simulations over a period of 2000 s. We start all of the simulated bacteria a distance of 173 μm away from the origin (173 μm is the distance between the original and final points obtained if one moves 100 μm along each axis), and the random walk brings the bacteria, on average, away from the origin at a rate of roughly 0.4 μm/s. Next, we add a stimulus to the simulation: we simulate the addition of 10 μM aspartate at the origin, such that the concentration falls off with increasing distance from the origin according to a

[3] A mechanistically interesting behavior in *E. coli* is the ability to thermotax, i.e., move up or down a thermal gradient (Imae et al., 1984; Maeda et al., 1976; Nara et al., 1991), possibly because of a temperature dependency in some or all of the rate coefficients.

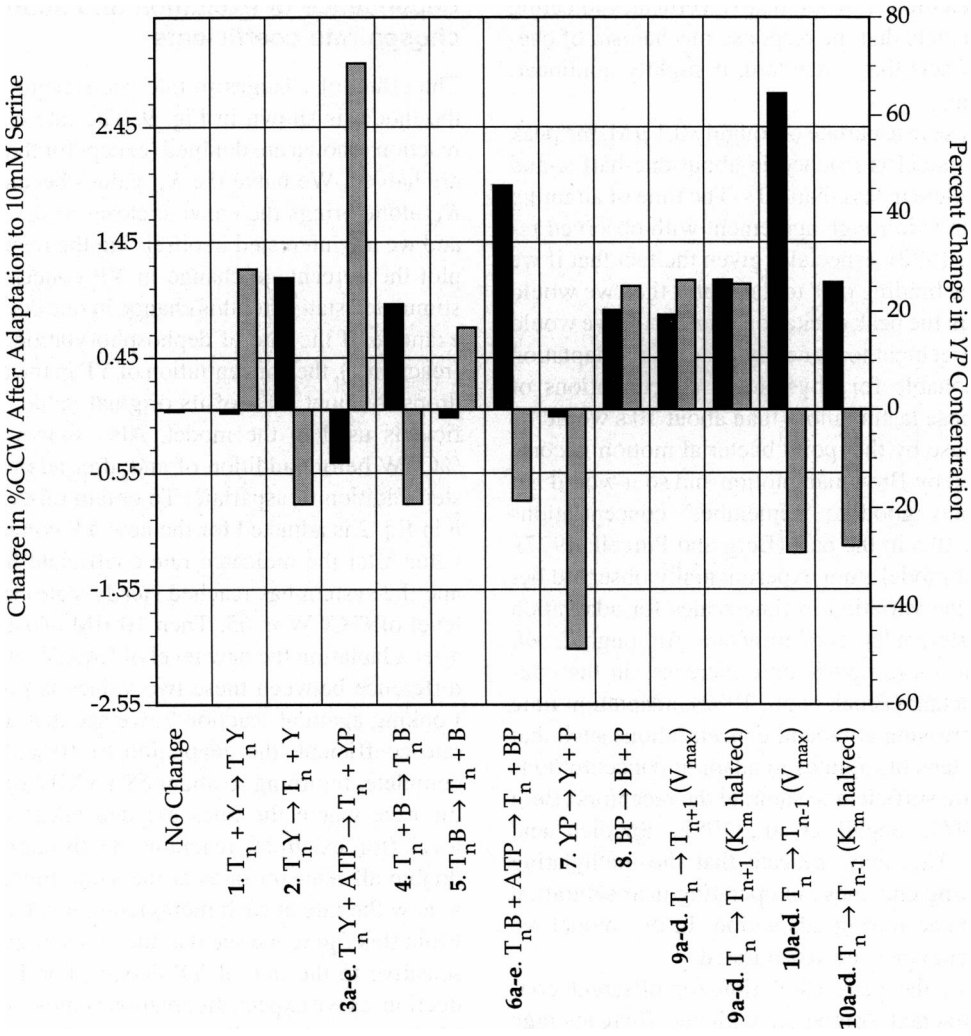

FIGURE 9 Plot showing the response of the model to changes in rate coefficients. For the indicated reaction, the rate coefficient or Michaelis constant is doubled (except K_M values, which are halved), and the resulting effect is shown. After the rate constant has been changed, the new steady-state concentration of YP is shown (*dotted bars*). The value of h in Eq. 2 is then adjusted to give a basal level of 65% CCW in the unstimulated state, and 10 μM aspartate is added. After adaptation is complete, the new fraction of CCW rotation is determined, and we plot the difference between the %CCW before and after the addition of aspartate (*solid bars*). We use this as an indicator of how the changes in rate coefficients affect adaptation.

normal curve with a SD of 160 μm. The concentration of aspartate at the starting point for the simulations (i.e., 173 μm away from the origin) was 5.6 μM. Fig. 10 *B* shows the mean distance from the origin we obtain by using the model for the chemotactic mechanism we have described. This behavior does not appear to be significantly different from that of bacteria where no attractant is present. Fig. 10 *C–F* illustrate the effect of increasing the Hill coefficient in Eq. 2 from 5.5 to 10 (*C*), 15 (*D*), 20 (*E*), and 50 (*F*). The chemotactic behavior of the model is enough to affect significantly the path of the simulated bacteria for a Hill coefficient of 15, and enough to keep the simulated bacteria in the vicinity of attractant for a Hill coefficient of 20.

A possible explanation of these results is that the model that we have developed is not sensitive enough to small changes in the fraction of receptors with attractant bound and, thus, the changes in %CCW rotation of the flagella caused by swimming up or down a gradient are insignificant compared with the "diffusion tendency" of the random walk. To investigate this possibility, we simulated a stepwise gradient of aspartate, where the concentrations decreased with increasing distance from the origin according to Table 2. Fig. 11 shows the results of this simulation, where we plot the mean behavior of 12 runs of the model in the absence of aspartate (*top curve*) and in the presence of the aspartate gradient described by Table 2 (*bottom curve*). In the presence of a stepwise gradient of aspartate, the model first moves toward the origin, and then remains, on average, about 80 μm away, indicating that the above explanation is likely to be valid.

CONCLUDING REMARKS

The agreement between experiments and the model presented here is very good in two important respects: (1) the time scale of the initial excitation is similar, and (2) the model gives exact adaptation to attractant, repellent, and any mixture of the two. However, the model fails to account for the

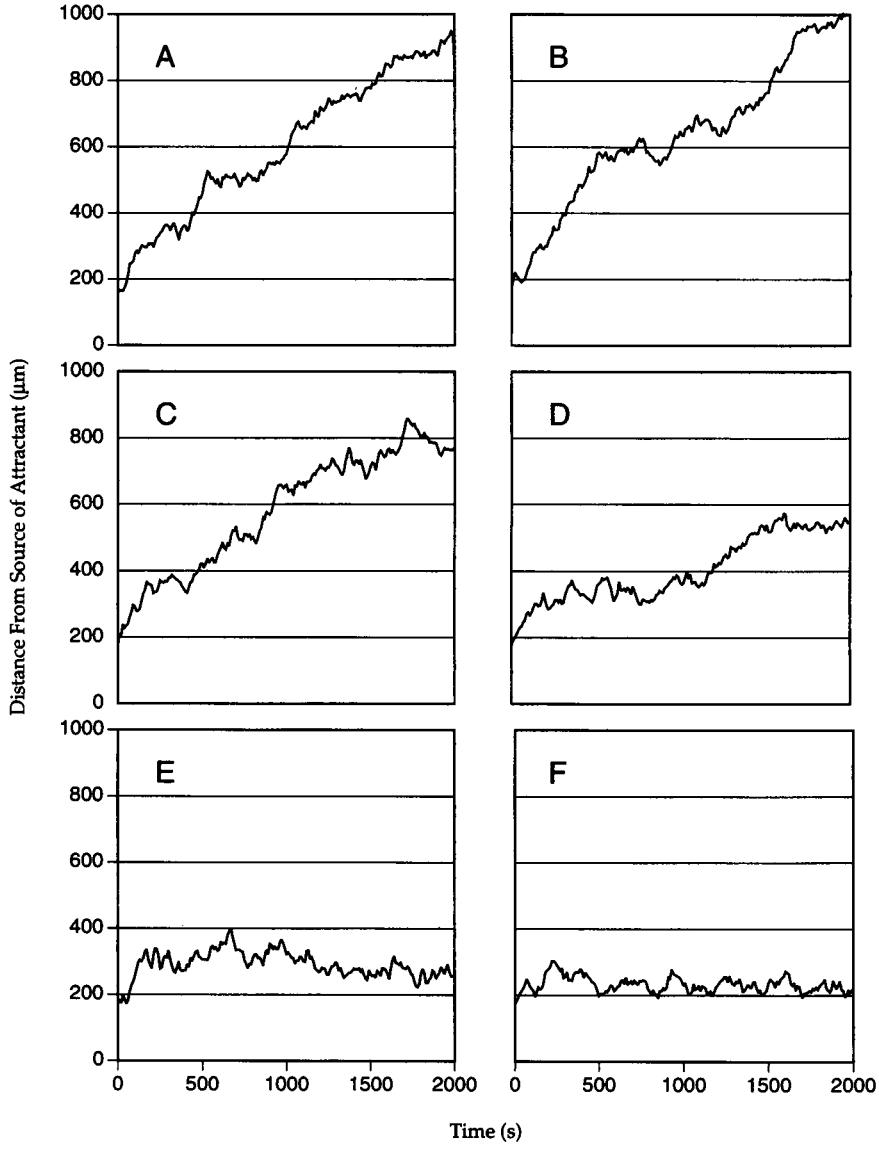

FIGURE 10 Plots showing the mean distances from the origin of five sets of simulations of the chemotactic behavior of our model versus time. (*A*) The mean distance of 12 runs versus time in the absence of stimulus (i.e., at all points, the concentration of aspartate is zero). (*B*) The mean distance of 12 runs versus time in the presence of an aspartate gradient. The aspartate gradient follows the normal distribution centered at the origin with a concentration of 10 μM aspartate and falling off with distance from the origin with a SD of 160 μm. The Hill coefficient for Eq. 2 in this simulation was the experimentally determined (Kuo and Koshland, 1989) value of 5.5. (*C*) The same as *B*, except with a Hill coefficient of 10, and 10 runs. (*D*) A Hill coefficient of 15 and 8 runs. Note that behavior is now significantly affected by the presence of the aspartate gradient. (*E*) A Hill coefficient of 20 and 7 runs. Note that the simulated bacteria now remain in the vicinity of the attractant. (*F*) A Hill coefficient of 50 and 10 runs.

TABLE 2 Concentrations of aspartate used in stepwise simulation

Distance (d) from origin (μm)	Asp concentration (μM)
$d \leq 25$	100
$25 < d \leq 50$	6.3
$50 < d \leq 75$	3.1
$75 < d \leq 100$	1.5
$100 < d \leq 125$	0.7
$125 < d \leq 150$	0.3
$150 < d \leq 175$	0.1
$175 < d \leq 200$	0.05
$d > 200$	0

See Fig. 11.

high sensitivity of bacterial chemotaxis. Also, in the model the time scale of adaptation does not depend significantly upon the concentration of stimulus added, whereas experiments have shown that *E. coli* take less time to adapt to small step increases in attractant concentration than they do to large step increases.

Adaptation is essential for efficient bacterial chemotaxis (Berg and Tedesco, 1975; Block et al., 1983; Stewart and Dahlquist, 1987; Weis et al., 1990). We have run simulations of chemotaxis (described in The Model) toward a point source of attractant using realistic mechanistic models, and have found that exact adaptation is extremely important to chemotaxis, and especially to the ability of a simulated bacterium to remain close to an attractant once it has approached the area (data not shown). Our model demonstrates exact adaptation. We have accomplished this by assuming that the concentration of BP returns to the basal level upon adaptation and, hence, this change is only a transient signal. Long term adaptation is accomplished through a change in the rate of methylation at the receptors with stimulatory ligand bound.

As demonstrated by Figs. 10 and 11, the largest discrepancy between the simulated behavior of our model and that of wild-type *E. coli* is the sensitivity to small changes in the fraction of receptors with attractant bound. Because this sensitivity is bounded by the limit $k_3 = 0$ with attractant bound,

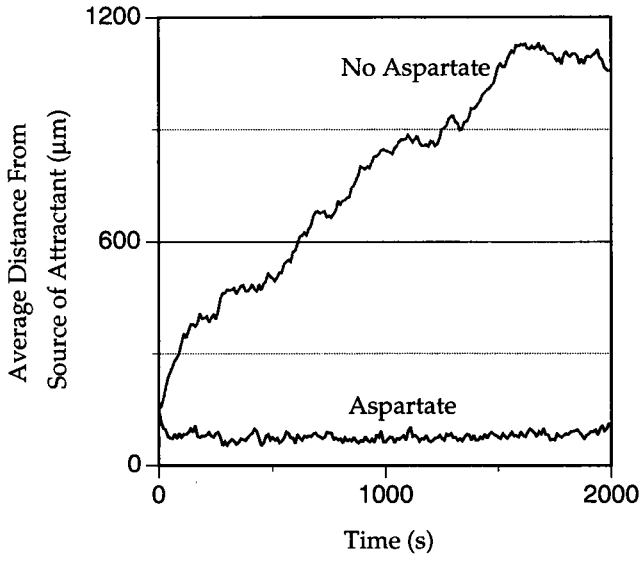

FIGURE 11 Plot showing the mean distance from the origin in simulations of the chemotactic behavior of our model versus time. The top curve (labeled "No Aspartate") shows the mean distance from the origin of 12 runs versus time in the absence of stimulus. The bottom curve (labeled "Aspartate") shows the mean distance from the origin of 12 runs versus time in the presence of a stepwise gradient of aspartate following the concentration distribution shown in Table 2. Note that the simulated bacteria first move toward the origin, and then remain on average about 80 μm away for the duration of the simulation. As the individual simulated bacteria undergo the weighted random walk, the variation in the distance from the origin is quite large, such that the SD of distance over a single run is about 35 μm.

it is unlikely that the reactions shown in Fig. 1 provide a complete mechanism for the chemotactic response. We believe that we have incorporated the available experimental evidence into our model and, therefore, that it is possible that an important mechanistic step is missing. An investigation into reactions that might increase the sensitivity of the response (and thus be similar to a change in the Hill coefficient in Eq. 2) would be of great help in understanding this system. Bray et al. (1993), for example, have suggested that receptors with attractants bound may stimulate the dephosphorylation of YP, although we found that by adding this reaction we were only able to improve sensitivity about 10-fold unless we allowed tens of minutes for adaptation to occur. This increase in sensitivity was not enough to affect significantly the chemotactic ability of the model. We could improve sensitivity more than 10-fold, but we were unable to find reasonable rate coefficients that enabled us to retain even nearly exact adaptation on a reasonable time scale. Allowing the steady-state concentration of PB to be dependent upon the concentration of attractant bound did not allow for sufficiently improved sensitivity either. Another possible mechanism of increasing sensitivity is the observed polymerization of the short form of CheA with the enzyme CheZ (which dephosphorylates YP), but this interaction and its effects are currently not well understood (H. Wang and P. Matsumura, personal communication).

Another deviation of our model from experiments is in the time scale of adaptation. Although the absolute time for adaptation may be decreased by changing the rate constants for methylation and demethylation, the variation in time scales poses a more difficult problem. We have had some success in adjusting the ratio that these time scales differ by altering the relative rates of methylation and demethylation for the different methylation states T. For instance, one may expect that if the methylation and demethylation rates between T_3 and T_4 are relatively slow, then it takes longer to adapt to large stimuli, because a disproportionate number of receptors must enter T_4 for adaptation to be complete if the stimulus is large. In a limited number of calculations, we have confirmed that the range of adaptation times can be increased by adjusting the relative rates of methylation, but the number of variables involved in obtaining exact adaptation for different relative rates of methylation and demethylation is large, and we have not looked deeply into this problem. Another possibility is that adaptation to a large stimulus is disproportionately slowed because of the transferase and esterase working near saturation, which may be reasonable given the number of molecules of each type in the cell. In this case, one may assume that a large stimulus saturates the enzymes and thus causes slower adaptation. We have done some work in this area by allowing the enzymes to operate at or near saturation, but the results were not conclusive.

Another question brought up by our model is the apparent nonessential role of BP. Even as a transient signal its role is not of major importance in our calculations (it serves to increase the rate of adaptation only about twofold), and its value does not change drastically after the addition of stimuli. Our assumptions then beg the question of why is there a significant phosphate flux through B if it is not essential to the task of adaptation. For a given rate of methylation and demethylation, adaptation in our model is slower if the concentration of BP is fixed than if it is allowed to change transiently. We may achieve the same rate of adaptation by increasing the rate of methylation and demethylation, but the transfer of a methyl group is more costly energetically than the transfer of a phosphate group, so it might be advantageous for the bacteria to minimize methyl transfers at the expense of increased phosphate flux.

As shown in Fig. 7, the chemotactic pathway acts as a slightly nonlinear adder. By this we mean that if the stimuli are added stepwise, the bacterium, in essence, calculates the difference in the fraction of receptors with attractant bound and those with repellent bound to determine its peak excitation. If there are more receptors with attractant bound, the initial response will be more smooth swimming, and if there are more receptors with repellent bound, the initial response will be more tumbling, with the exact changes in fraction CCW rotation of the individual flagella determined by the difference between the two values. This is a surprisingly simple result and does not appear to be merely an artifact of the specific rate constants chosen.

We thank Professor Lubert Stryer for suggesting this study and for many helpful and stimulating discussions.
This work was supported in part by the Department of Energy/Basic Energy Sciences.

REFERENCES

Arkin, A., and J. Ross. 1994. Computational functions in biochemical reaction networks. *Biophys. J.* 67:560–578.

Berg, H. C., and D. Brown. 1972. Chemotaxis in *Escherichia coli* analyzed by three dimensional tracking. *Nature.* 239:500–504.

Berg, H. C., and E. M. Purcell. 1977. Physics of chemoreception. *Biophys. J.* 20:193–219.

Berg, H. C., and P. M. Tedesco. 1975. Transient response to chemotactic stimuli in *Escherichia coli*. *Proc. Natl. Acad. Sci. USA.* 72:3235–3239.

Block, S. M., J. E. Segall, and H. C. Berg. 1982. Impulse responses in bacterial chemotaxis. *Cell.* 31:215–226.

Block, S. M., J. E. Segall, and H. C. Berg. 1983. Adaptation kinetics in bacterial chemotaxis. *J. Bacteriol.* 154:312–323.

Borczuk, A., A. Staub, and J. Stock. 1986. Demethylation of bacterial chemoreceptors is inhibited by attractant stimuli in the complete absence of the regulatory domain of the demethylating enzyme. *Biochem. Biophys. Res. Commun.* 141:918–923.

Borkovich, K. A., L. A. Alex, and M. I. Simon. 1992. Attenuation of sensory receptor signaling by covalent modification. *Proc. Natl. Acad. Sci. USA.* 89:6756–6770.

Borkovich, K. A., N. Kaplan, J. F. Hess, and M. I. Simon. 1989. Transmembrane signal transduction in bacterial chemotaxis involves ligand-dependent activation of phosphate group transfer. *Proc. Natl. Acad. Sci. USA.* 86:1208–1212.

Borkovich, K. A., and M. I. Simon. 1990. The dynamics of protein phosphorylation in bacterial chemotaxis. *Cell.* 63:1339–1348.

Bourret, R. B., K. A. Borkovich, and Simon. 1991. Signal transduction pathways involving protein phosphorylation in prokaryotes. *Annu. Rev. Biochem.* 60:401–441.

Bourret, R. B., J. F. Hess, and M. I. Simon. 1990. Conserved aspartate residues and phosphorylation in signal transduction by the chemotaxis protein CheY. *Proc. Natl. Acad. Sci. USA.* 87:41–45.

Bray, D., R. B. Bourret, and M. I. Simon. 1993. Computer simulation of the phosphorylation cascade controlling bacterial chemotaxis. *Mol. Cell. Biol.* 4:469–482.

Corana, A., M. Marches, C. Martini, and S. Ridella. 1987. Minimizing multimodal functions of continuous variables with the "simulated annealing" algorithm. *ACM Trans. Math. Software.* 13:262–280.

Dowling, J. E., and H. Ripps. 1970. Visual adaptation in retina of the skate. *J. Gen. Physiol.* 56:499–520.

Engström, P., and G. L. Hazelbauer. 1980. Multiple methylation of methyl-accepting chemotaxis proteins during adaptation of *E. coli* to chemical stimuli. *Cell.* 20:165–171.

Foster, D. L., S. L. Mowbray, B. K. Jap, and D. E. Koshland. 1985. Purification and characterization of the aspartate chemoreceptor. *J. Biol. Chem.* 260:11706–11710.

Gegner, J. A., D. R. Graham, A. F. Roth, and F. W. Dahlquist. 1992. Assembly of an MCP receptor, CheW, and kinase CheA complex in the bacterial chemotaxis signal transduction pathway. *Cell.* 70:975–982.

Hazelbauer, G. L., C. Park, and D. M. Nowlin. 1989. Adaptational "crosstalk" and the crucial role of methylation in chemotactic migration by *Escherichia coli*. *Proc. Natl. Acad. Sci. USA.* 86:1448–1452.

Hess, J. F., K. Oosawa, N. Kaplan, and M. I. Simon. 1988. Phosphorylation of three proteins in the signalling pathway of bacterial chemotaxis. *Cell.* 53:79–87.

Hjelmfelt, A., and J. Ross. 1992. Chemical Implementation and Thermodynamics of Collective Neural Networks. *Proc. Natl. Acad. Sci. USA.* 89:388–391.

Hjelmfelt, A., and J. Ross. 1993. Pattern Recognition, Chaos, and Multiplicity in Neural Networks of Excitable Systems. *Proc. Natl. Acad. Sci. USA.* 91:63–67.

Hjelmfelt, A., F. W. Schneider, and J. Ross. 1993. Pattern recognition in coupled chemical kinetic systems. *Science.* 260:335–337.

Hjelmfelt, A., E. D. Weinberger, and J. Ross. 1991. Chemical implementation of neural networks and turing machines. *Proc. Natl. Acad. Sci. USA.* 88:10983–10987.

Hjelmfelt, A., E. D. Weinberger, and J. Ross. 1992. Chemical implementation of finite state machines. *Proc. Natl. Acad. Sci. USA.* 89:383–387.

Imae, Y., T. Mizuno, and K. Maeda. 1984. Chemosensory and thermosensory excitation in adaptation-deficient mutants of *Escherichia coli*. *J. Bacteriol.* 159:368–374.

Ishihara, A., J. E. Segall, S. M. Block, and H. C. Berg. 1983. Coordination of flagella on filamentous cells of *E. coli*. *J. Bacteriol.* 155:228–237.

Kehry, M. R., T. G. Doak, and F. W. Dahlquist. 1984. Stimulus-induced changes in methylesterase activity during chemotaxis in *E. coli*. *J. Biol. Chem.* 259:11828–11835.

Kleene, S. J., A. C. Hobson, and J. Adler. 1979. Attractants and repellents influence methylation and demethylation of methyl-accepting chemotaxis proteins in an extract of *E. coli*. *Proc. Natl. Acad. Sci. USA.* 76: 6309–6313.

Knox, B. E., P. N. Devreotes, A. Goldbeter, and L. A. Segel. 1986. A molecular mechanism for sensory adaptation based on ligand-induced receptor modification. *Proc. Natl. Acad. Sci. USA.* 83:2345–2349.

Koshland, D. E. 1988. Chemotaxis as a model second-messenger system. *Biochemistry.* 27:5829–5833.

Kuo, S. C., and D. E. Koshland. 1987. Roles of CheY and CheZ gene products in controlling flagellar rotation in bacterial chemotaxis of *E. coli*. *J. Bacteriol.* 169:1307–1314.

Kuo, S. C., and D. E. Koshland. 1989. Multiple kinetic states for the flagellar motor switch. *J. Bacteriol.* 171:6279–6287.

Larsen, S. H., R. W. Reader, E. N. Kort, W. Tso, and J. Adler. 1974. Change in direction of flagellar rotation is the basis of the chemotactic response in *E. coli*. *Nature.* 249:74–77.

Leifson, E. 1960. Atlas of Bacterial Flagellation. Academic Press, New York.

Lupas, A., J. Stock, R. M. MacNab, and D. P. Han. 1983. Phosphorylation of an n-terminal regulatory domain activates the CheB methylesterase in bacterial chemotaxis. *Cell.* 32:109–117.

Maeda, K., Y. Imae, J.-I. Shioi, and F. Oosawa. 1976. Effect of temperature on motility and chemotaxis of *E. coli*. *J. Bacteriol.* 127:1039–1046.

Matsumura, P., S. Roman, K. Bolz, and D. McNally. 1990. Signalling complexes in bacterial chemotaxis. *Symp. Soc. Gen. Microbiol.* 188:135–154.

McNally, D. F., and P. Matsumura. 1991. Bacterial chemotaxis signaling complexes: formation of a chea/chew complex enhances autophosphorylation and affinity for CheY. *Proc. Natl. Acad. Sci. USA.* 88:6269–6273.

Metropolis, N., A. Rosenbluth, M. Rosenbluth, A. Teller, and E. Teller. 1953. Equation of State calculations by fast computing machines. *J. Chem. Phys.* 21:1087–1092.

Mowbray, S. L., and D. E. Koshland. 1987. Additive and independent responses in a single receptor: aspartate and maltose stimuli on the Tar protein. *Cell.* 50:171–180.

Nara, T., L. Lee, and Y. Imae. 1991. Thermosensing ability of Trg and Tap chemoreceptors in *E. coli*. *J. Bacteriol.* 173:1120–1124.

Ninfa, E. G., A. Stock, S. Mowbray, and J. Stock. 1991. Reconstitution of the bacterial chemotaxis signal transduction system from purified components. *J. Biol. Chem.* 266:9764–9770.

Parkinson, J. S. 1993. Signal transduction schemes of bacteria. *Cell.* 73: 857–871.

Ravid, S., P. Matsumura, and M. Eisenbach. 1986. Restoration of flagellar clockwise rotation in bacterial envelopes by insertion of the chemotaxis protein CheY. *Proc. Natl. Acad. Sci. USA.* 83:7157–7161.

Russell, C. B., R. C. Stewart, and F. W. Dahlquist. 1989. Control of transducer methylation levels in *Escherichia coli*: investigation of components essential for modulation of methylation and demethylation reactions. *J. Bacteriol.* 175:3609–3618.

Sanders, D. A., and D. E. Koshland. 1988. Receptor interactions through phosphorylation and methylation pathways in bacterial chemotaxis. *Proc. Natl. Acad. Sci. USA.* 85:8425–8429.

Schuster, S. C., R. V. Swanson, L. A. Alex, R. B. Bourret, and M. I. Simon. 1993. Assembly and function of a quaternary signal transduction complex monitored by surface plasmon resonance. *Nature.* 365:343–346.

Segall, J. E., S. M. Block, and H. C. Berg. 1986. Temporal comparisons in bacterial chemotaxis. *Proc. Natl. Acad. Sci. USA.* 83:8987–8991.

Segall, J. E., M. D. Manson, and H. C. Berg. 1982. Signal processing times in bacterial chemotaxis. *Nature.* 296:855–857.

Segel, L. A., A. Goldbeter, P. N. Devreotes, and B. E. Knox. 1986. A mechanism for exact sensory adaptation based on receptor modification. *J. Theor. Biol.* 120:151–179.

Silverman, M., and M. I. Simon. 1974. Flagellar rotation and the mechanism of bacterial motility. *Nature.* 249:73–74.

Silverman, M., and M. I. Simon. 1977. Chemotaxis in *Escherichia coli*: methylation of *che* gene products. *Proc. Natl. Acad. Sci. USA.* 74:3317–3321.

Simms, S. A., A. M. Stock, and J. B. Stock. 1987. Purification and characterization of the s-adenosylmethionine: glutamyl methyltransferase that modifies membrane chemoreceptor proteins in bacteria. *J. Biol. Chem.* 262:8537–8543.

Springer, M. S., M. P. Goy, and J. P. Adler. 1977. Sensory transduction in *Escherichia coli*: two complimentary pathways of information processing that involve methylated proteins. *Proc. Natl. Acad. Sci. USA.* 74:3312–3316.

Spudich, J. L., and D. E. Koshland, Jr. 1975. Quantation of the sensory response in bacterial chemotaxis. *Proc. Natl. Acad. Sci. USA.* 72: 710–713.

Stewart, R. C., and F. W. Dahlquist. 1987. Molecular components of bacterial chemotaxis. *Chem. Rev.* 87:997–1025.

Stock, J. B., G. S. Lukat, and A. M. Stock. 1991. Bacterial chemotaxis and the molecular logic of intracellular signal transduction networks. *Annu. Rev. Biophys. Biophys. Chem.* 20:109–136.

Stock, J. B., A. J. Ninfa, and A. M. Stock. 1989. Protein phosphorylation and regulation of adaptive responses in bacteria. *Microbiol. Rev.* 53: 450–490.

Terwilliger, T. C., J. Y. Wang, and D. E. Koshland, Jr. 1986. Kinetics of receptor modification. *J. Biol. Chem.* 261:10814–10820.

Toews, M. L., M. F. Goy, M. S. Springer, and J. Adler. 1979. Attractants and repellents control demethylation of methylated chemotaxis proteins in *Escherichia coli*. *Proc. Natl. Acad. Sci. USA.* 76: 5544–5548.

Tso, W., and J. Adler. 1974. Negative chemotaxis in *Escherichia coli*. *J. Bacteriol.* 118:560–576.

Weis, R. M., S. Chassalow, and D. E. Koshland, Jr. 1990. The role of methylation in chemotaxis, an explanation of outstanding anomalies. *J. Biol. Chem.* 265:6917–6826.

Weis, R. M., and D. E. Koshland, Jr. 1990. Chemotaxis in *Escherichia coli* proceeds efficiently from different initial tumble frequencies. *J. Bacteriol.* 172:1099–1105.